Frequency-Reconfigurable Multi-band MIMO Antenna Using Gradient Structure for IoT

Duong Thi Thanh Tu and Nguyen Van Sang
Faculty of Telecommunication 1, Posts and Telecommunications Institute of Technology, Hanoi, Vietnam

Corresponding author: Duong Thi Thanh Tu (e-mail: tudtt@ ptit.edu.vn).

ABSTRACT A frequency reconfigurable multi-band MIMO antenna is presented in this study. The single antenna consists of only one PIN diode that can change antenna operating frequencies between two different quad-bands. Their bands not only cover the popular NB-IoT bands such as 900MHz, 1.8GHz, and 2.4GHz for Z-Wave, ZigBee, RFID, GSM communication but also contain 5G IoT bands. They are 2.4GHz, 2.6 GHz, and 5GHz for LTE-A, 802.11n, ac, and 5G below 10GHz. Based on the complex structure of the ring and new moon shape, the single antenna achieves a compact size of 30 mm x 30 mm x 1.6 mm. This volume is about 76% reduction compared to a conventional ring antenna at 900MHz. Additionally, a structure of gradient arcs is proposed to decrease mutual coupling among closed-spaced elements of MIMO antenna for the distance of 0.033λ at the lower band from edge to edge. The proposed antennas are analyzed using CST software, measured using a VNA, and used with an IEEE 802.11 USB adapter. The simulated, measured, and experimental results agree well.

INDEX TERMS Reconfigurable, MIMO, IoT, mutual coupling.

I. INTRODUCTION

AT present, reconfigurable antennas play a major role in modern wireless communication systems because of many advantages such as multifunctional capabilities, compact volume size, low front-end processing efforts, and good isolation [1], [2]. There are several types of reconfigurable antennas such as frequency, bandwidth, radiation pattern, and polarization reconfiguration. There are also different ways to change antenna operation by switches, for example, RF micro electro mechanical systems (MEMS), varactor diode, and PIN diode. However, PIN diode switches are preferred in reconfigurable antenna designs because of their small size, low cost, and fast switching [2]. Different types of reconfigurable multiband antennas have been developed for modern wireless systems in recent years [2]-[8]. T. Khan *et al.* [3] presented a multiband frequency reconfigurable antenna with four PIN diodes for four states but there are the same resonant frequencies at the different states such as 2.7GHz, 4.7GHz, and 5.4GHz bands. The antenna size is 40 x 60 x 1.6 mm^3 and the lowest resonant frequency is 2.7GHz. Thus it is not a small antenna. Having the same operating frequency in the different modes is also the drawback of J. Kumar *et al.* [4], H. F. Abutarboush, and A. Shamim [5], and Saffrine Kingsly et al. [6]. Getting a compact size is one of the advantages of the reconfigurable antenna but it is not easy to be fitted on a small form-factor like IoT devices if the antenna provides sub-GHz operating frequencies. That is the reason that there are many reconfigurable multiband antennas lacking a 900MHz band [3], [5]-[8].

On the other hand, Multiple Input Multiple Output (MIMO) antennas are becoming an integral part of all digital communication systems [9]. MIMO technology provides higher data throughput without increasing transmit power or spectrum. The main disadvantage of the MIMO antenna is the mutual coupling between close antenna elements. In recent years, various isolation techniques were introduced to reduce the mutual coupling. However, most of them concentrated on single-band MIMO antennas, several ones affected multiband MIMO antennas, and a few ones studied for frequency reconfigurable MIMO antennas [10]-[12]. M.M. Hassan *et al.* [10] have proposed a 1x2 frequency reconfigurable MIMO antenna using RF MEMS switches. The antenna can operate at two or three of five bands at different states but at all cases of switching, the antenna isolation cannot satisfy the modern MIMO standard of over 20dB at 5.5GHz operating frequency. It is the same for S. R. Thummaluru *et al.* [11]. Their 2x2 MIMO antenna gets standard isolation of over 20dB at 2.4GHz-2.5 GHz band but falls to 15dB at 5.1GHz-5.8GHz one. S. Riaz *et al.* [12] has decreased 6dB mutual coupling by using DGS but the isolation gets only 12dB for all bands of 1x2 MIMO antenna.

In this paper, we propose a frequency reconfigurable quad-band MIMO antenna for IoT devices. Based on a complex structure of ring and new moon, our antenna not only gets a compact size that can be fitted on a small form-factor but also operates at a sub-GHz band. To decrease the mutual coupling between the close antenna elements, a structure of gradient arcs is proposed. At all eight operating

bands, the antenna isolation is over 20dB that can meet the isolation demand of good MIMO antenna.

The rest of this paper is organized as follows. In Part II and Part III, the single and MIMO antenna designs are presented, respectively. Simulated and measured results as well as their analysis are also studied in these Parts. The experimental results with the IEEE 802.11 USB Adapter are shown in Part IV. Finally, Part V concludes the study.

II. SINGLE ANTENNA

A. ANTENNA STRUCTURE

In general, the effective length of the radiator has a significant role determining the operating frequency of the antenna. Thus, one of the common methods to create a frequency-reconfigurable antenna is changing the electrical length by switching [13]. In this paper, we use only one PIN diode switch to control two different shapes on the radiating element to vary the electrical length. Thus, the operating frequencies are able to be switched from a quad-band to another.

As shown in Fig.1, the structure of the proposed-single antenna includes three parts: A radiating patch based on a complex shape of a ring and a new moon, defected ground, and one PIN diode connecting the ring structure and the new moon one. Based on the FR4 substrate with a dielectric constant of 4.3 and a thickness of 1.6 mm, the antenna dimension is calculated and optimized by CST software and presented in Table I. The antenna is rather compact with the total size of 30x30x1.6mm^3.

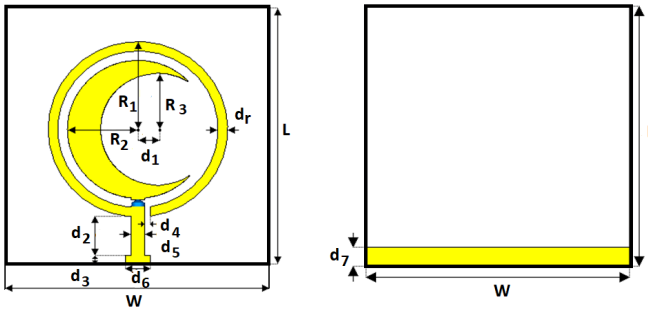

(a) Top view (b) Bottom view

FIGURE 1. The geometry of the proposed-single antenna

TABLE I. The dimensions of the proposed-single antenna

Parameter	Size (mm)	Parameter	Size (mm)
W	30	d_1	2
L	30	d_2	4.5
R_1	10.2	d_3	1
R_2	8.1	d_4	1
R_3	6.6	d_5	2
d_r	1.1	d_6	2.9
d_7	3		

1) DESIGN OF RADIATING ANTENNA

The radiating element is a complex structure that consists of a ring shape and a new moon shape with four different radii to determine the different resonant modes. Firstly, we calculate roughly these radii by using the method of disk antenna because they have the same type of radiation fields [14]. Then, these radii are optimized by CST software.

For the TM_{nm} mode, the resonant frequency of a disk antenna can be evaluated from Equation 1.

$$f_{nm} = \frac{X_{nm}c}{2\pi a_e\sqrt{\epsilon_r}} \quad (1)$$

where c is the speed of light in a vacuum, a_e is the effective radius, and ε_r is the dielectric constant of the substrate. X_{nm} is the m^{th} zero of Bessel function of order n $Jn'(ka)$. It is proven that the dominant mode that is the mode corresponding to $n=m=1$ has a minimum radius or resonant frequency. Hence we choose TM_{11} mode to determine the radius of a disk (a_e) for a given resonant frequency by Equation 2:

$$a_e = a\left\{1 + \frac{2h}{\pi a\varepsilon_r}\left(ln\frac{\pi a}{2h} + 1.7726\right)\right\}^{1/2} \quad (2)$$

where h is the thickness of dielectric, a is calculated from the basic relation in Equation 3:

$$X_{nm} = ka \quad (3)$$

and k is determined by Equation 4:

$$k = \frac{2\pi\sqrt{\varepsilon_r}}{\lambda_0} \quad (4)$$

2) PIN DIODE SWITCHING

As shown in Fig.1, we use only one PIN diode to be the switching element connecting two parts of the radiation patch: the ring structure and the new moon one. In our antenna design, Beam Lead PIN diode MA4AGBLP912 is chosen because this PIN diode has a low insertion loss, fast switching rate, small size, and also wide operating bandwidth. The PIN diode can be turned on and off by using suitable polarity voltage. The ON and OFF states of the PIN MA4AGBLP912 diode via inductor L, resistance R_S, R_P, and capacitor C_T are illustrated in Figure 2.

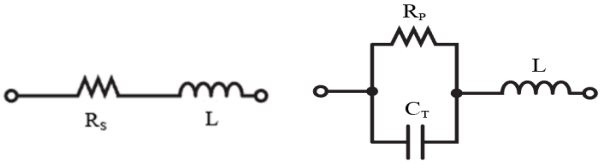

(a) ON state (b) OFF state

FIGURE 2. Equivalent circuit of Beam Lead PIN diode

The ON state is achieved by series resistor R_S with inductor L while the OFF state is made by parallel resistor R_P with the capacitor C_T then connected in series with the inductor L. The values of L, R_S, R_P, and C_T in the two on-off states are described in Table II. It is obvious that the lower value of R_S in the RL circuit allows current flow from the feeding line to the radiating patches and the higher value of R_P, C_T in RLC circuit prevents the current from flowing between the radiating patch and feeding line.

TABLE II. Parameters of PIN MA4AGBLP912 diode

Parameters	L	C_T	R_S	R_P
Value	0.5nH	0.025pF	4Ω	10kΩ

B. SIMULATION RESULTS AND ANALYSIS

The performance of the proposed reconfigurable multiband antenna is validated by CST simulation software. In this section, the single antenna characteristics are studied in terms of reflection coefficient, current density, and radiation pattern.

1) REFLECTION COEFFICIENT

The reflection coefficient results (S11) of the designed antenna under ON and OFF states of the PIN diode are presented in Fig.3. The proposed antenna is a quad-band antenna in both states. In the OFF state, the antenna operates at four bands of 2.45GHz, 3.3GHz, 5.5GHz, and 8.2GHz. Their bandwidth are 240MHz (9.8%), 320MHz (9.7%), 520MHz (9.4%), and 650MHz (7.8%), respectively. In the ON state, four resonant frequencies of the antenna are 0.92GHz, 1.8GHz, 2.6GHz, and 5GHz. Their bandwidth are 40MHz (4.3%), 90MHz (5%), 550MHz (21%), and 750MHz (15%), respectively. Thus, the proposed antenna can operate at the eight different bands. These bands cover both popular NB-IoT bands such as 900MHz, 1.8GHz, 2.4GHz for Z-Wave, ZigBee, RFID, GSM communication, and 5G IoT bands which are 2.4GHz, 2.6 GHz, and 5GHz for LTE-A, 802.11n, ac, and 5G below 10GHz.

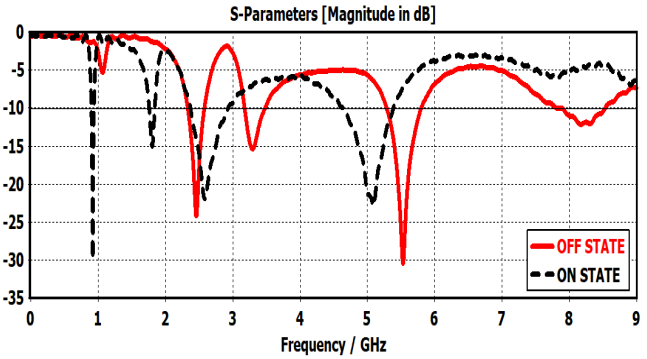

FIGURE 3. Simulated coefficient of the single antenna at different states

2) CURRENT DENSITY ANALYSIS

To explain the working principle intuitively, the simulation of surface current distribution is presented in Fig.4.

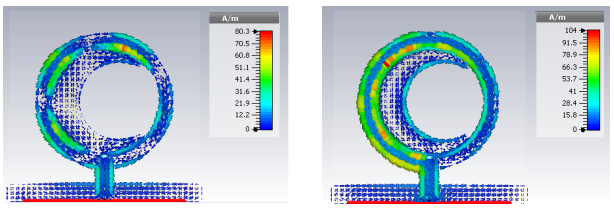

(a) OFF state (b) ON state

FIGURE 4. Current distribution on the radiating patch

Based on the switching from OFF state to ON state of the PIN diode, the shape of the radiating patch is increased. Thus the operating frequencies are decreased as shown in Table III. That is why the proposed antenna can achieve the sub-GHz band with a compact size.

TABLE III. Comparison of two switching states

Antenna switching state	PIN diode	Shape of radiating patch	Operating frequency (GHz)
State 1	OFF	Ring shape	2.4; 3.3; 5.5; 8.2
State 2	ON	Ring and new moon shape	0.9; 1.8; 2.6; 5

We can determine these operating frequencies of the proposed antenna through current density analysis as well as an approximate calculation using Equation 1. The highest band of the proposed antenna is achieved when the electrical current concentrates on the inner curve of the moon shape. It is calculated as following:

$$f_H = \frac{1.84118 * 3.10^8}{2\pi * (6.6 * 3/4).10^{-3} * \sqrt{4.3}} = 8.56\text{GHz} \quad (5)$$

The antenna will get the lowest operating frequency when the electrical current flows from the feeding line to concentrates not only on the inner and outer of the ring shape but also on both sides of the moon one. This frequency is computed as follow:

$$f_L = \frac{1.84118 * 3.10^8}{2\pi * (6.6 + 8.1 + 9.1 + 10.2 + 4.5 * 2).10^{-3} * \sqrt{4.3}} = 0.985\text{GHz} \quad (6)$$

At the same analysis, we can see that the proposed antenna can operate at different bands via the varied electric current concentration on the radiation patch. That is why the antenna can make a multi-band operation. All frequencies can be determined as the above calculation. We also can calculate the ratio of our antenna size to a traditional disk antenna. With the same radius of the outer ring, the resonant frequency of a conventional disk antenna can be calculated as follow:

$$f_{disk} = \frac{1.84118 * 3.10^8}{2\pi * (10.2).10^{-3} * \sqrt{4.3}} = 4.156\text{GHz} \quad (7)$$

Thus, the ratio of our antenna size to a conventional disk antenna one is:

$$R = 0.985/4.156 = 0.237 = 23.7\% \quad (8)$$

That means the proposed antenna gains a 76.3% reduction compared to a conventional disk antenna.

3) RADIATION PATTERN

Fig.5 shows the simulated radiation patterns of the proposed reconfigurable antenna at eight different resonant frequencies in two states. It is obvious that the dipole polarization can achieved in all bands.

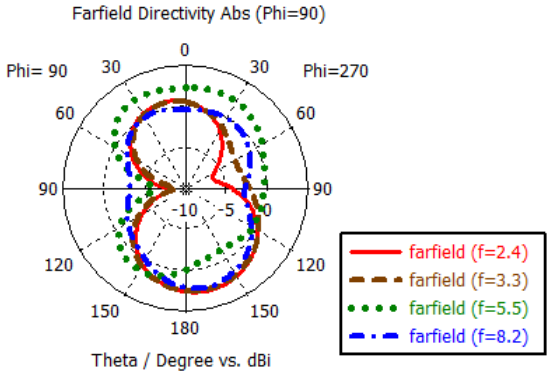

(a) OFF state

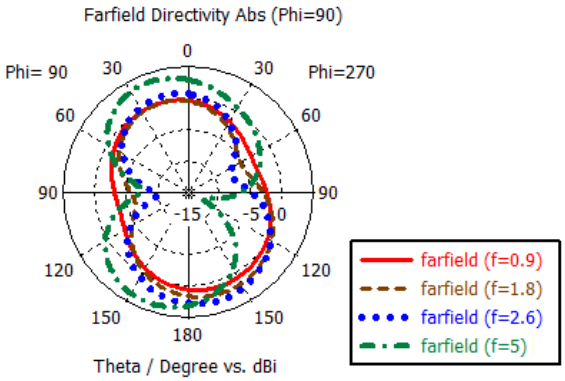

(b) ON state

FIGURE 5. Radiation pattern of the proposed single antenna

4) COMPARISON

The proposed antenna is compared with some other recently reported multiband reconfigurable antennas as shown in Table IV.

TABLE IV. Performance Comparison of the proposed single antenna and recently published work

REF	Size (mm^2)	Substrate	Height (mm)	No of operating band	Reconfigurable state/ Switches	Center Frequency (GHz)
[3]	2400	FR4	1.6	12	4/4	2.7; 4.1; 4.2; 4.4; 5.4; 6.6; 6.9; 8.1; 8.4; 8.6; 8.8; 9.4
[4]	2500	FR4	3.2	5	3/6	0.85/0.9; 1.6; 1.7; 1.8; 2.4
[5]	900	Photo paper	0.44	5	4/2	1.6; 2.5; 2.9; 3.1; 3.5
[6]	1800	FR4	1.6	4	4/5	1.8; 2.4; 3.5; 5.2
[7]	10395	RO5880	0.6	8	2/4	1.57-2.15;2.13-3.0;3.17-3.43; 5.2-5.8;6.3-6.78;8.31-8.90;9.04-9.58;12-13.14
[8]	2500	FR4	1.6	4	2/4	4.5; 3.5; 2.4; 1.8
This work	900	FR4	1.6	8	1/2	0.9; 1.8; 2.4; 2.6; 3.3; 5; 5.5; 8.2

It can be noted that there is no sub-GHz band in the operating frequencies of many above antennas [3], [5]-[8] while the total size is larger than the proposed antenna. Though the antenna in [4] operates at 850/ 900MHz, its volume is nearly three-time greater than our design. Besides, at the same number of operation bands, the proposed antenna uses a minimum ratio of the number of switches and resonances so it can decrease the losses which are incurred by the switches as well as reduce the complexity level of the design.

C. MEASUREMENT

The proposed antenna is fabricated and measured. Based on the FR4 substrate with a height of 1.6mm, the fabricated antenna has a compact size of 30x30x1.6mm^3 as shown in Fig.6. The Beam Lead PIN diode MA4AGBLP912 is used to be a switch to ensure a minimum insertion loss.

The measured reflection coefficient of the proposed antenna at differential modes is compared to simulated ones in Fig. 7. It is obvious to see that the measured results are quite similar to the simulated ones. The fabricated antenna can operate at eight different frequencies as in the simulated results and can switch from a quad-band operation to another. The reason is an impedance variation by inserting the power supply for the diode on the fabricated antenna. For S11<-10dB, the frequency reconfigurable antenna achieves an impedance bandwidth in (980-1050)MHz, (2.56-2.88)GHz, (3.4-3.988)GHz, (5.2-5.76) GHz, and (7.4-9)GHz at the OFF State; (840-960)MHz, (1.8-2)GHz, (2.6-3.68)GHz, (4.24-5.32)GHz, and (7.4-9)GHz at the ON state.

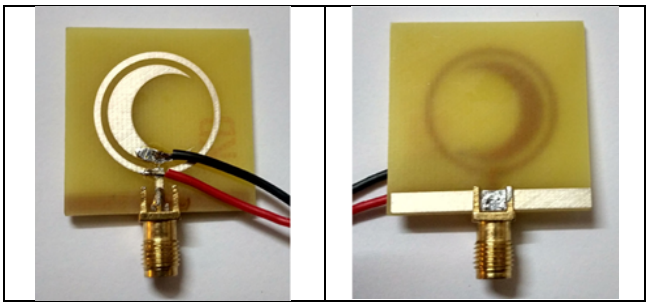

(a) Top view (b) Bottom view

FIGURE 6. Fabricated reconfigurable antenna

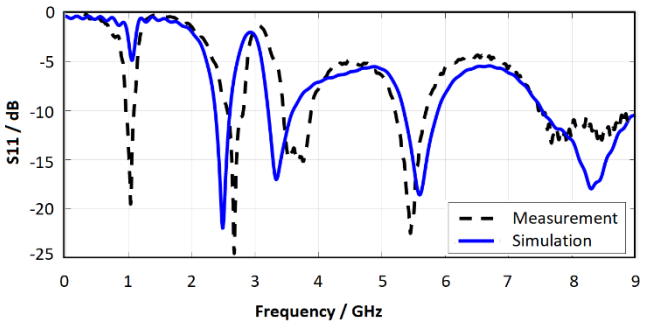

(a) OFF state

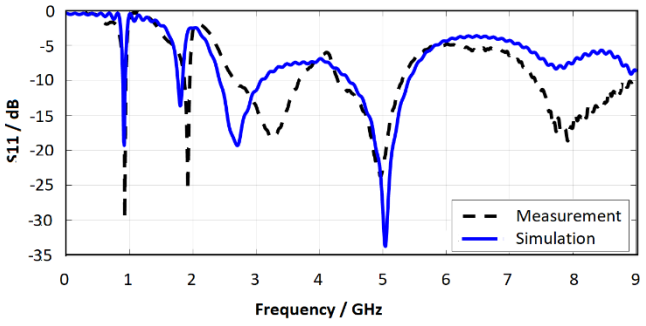

(b) ON state

FIGURE 7. The simulated and measured reflection coefficient of the single antenna

III. MIMO ANTENNA

A. DESIGN OF MIMO ANTENNA

The frequency reconfigurable multi-band MIMO antenna is constructed by placing two single antennas side by side at a close distance of 41mm (0.123λ at 900MHz) from feeding point to feeding point. From edge to edge, it is 11mm that is equal to 0.033λ at 900MHz (the lowest resonant frequency of the proposed antenna). The total size of the antenna is 71 x 30 x 1.6 mm^3. To decrease the mutual coupling between two close antenna elements at both operating bands, a novel structure of adjacent arcs on the surface plane is proposed as illustrated in Figure 8 where R=13.5mm and D=16mm, d=0.5mm.

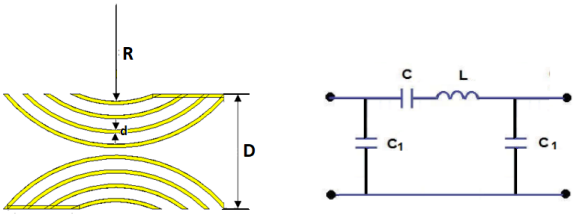

(a) Design (b) Equivalent circuit

FIGURE 8. The proposed decoupling structure based on gradient arcs

Thus, the radius of adjacent arcs is increased steadily with the distance between the curves of 1.5mm. The equivalent circuit of the proposed structure includes a capacitor C, an inductance L, and two capacitor C1 where C is the sum of C_i (i is from 1 to n) that is the gap capacitance between adjacent arcs, C_1 is formed by metal line of surface and ground plane. L is the equivalent inductance that is made of the metal arc in the surface plane.

The transfer function of the equivalent circuit of adjacent arcs is calculated by Equation 9 and shown in Fig.9. It is seen that this structure behaves as a band-pass filter at low frequency and a stop band at the high band. At $f>f_c$ where f_c is determined by Equation (10), no wave can pass through the structure of adjacent arcs. That is why this structure can reduce mutual coupling between two antenna elements for a wideband covering all eight antenna bands.

$$H(jw) = \frac{U_{out}}{U_{in}} = \frac{1}{\left(1+\frac{C_1}{C}\right)\left(1-w^2\frac{LCC_1}{C+C_1}\right)} \tag{9}$$

$$f_c = \frac{1}{2\pi}\sqrt{\frac{C+C_1}{LCC_1}} \tag{10}$$

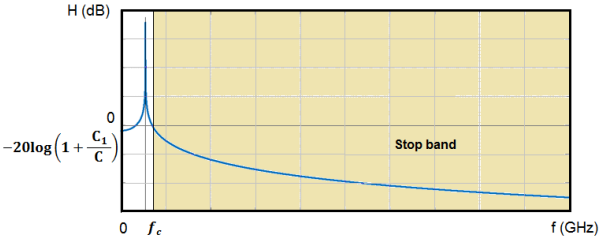

FIGURE 9. The magnitude of the frequency response of the proposed decoupling structure

The frequency reconfigurable multi-band MIMO antenna using the gradient arc structure is shown in Fig.10. There is a small change in the size of the MIMO antenna in order to fit the decoupling structure between the radiating elements. Thus, the total size of the antenna is 71 x 30.78 x 1.6 mm^3.

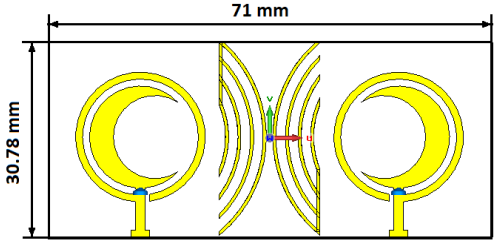

(a) Top view

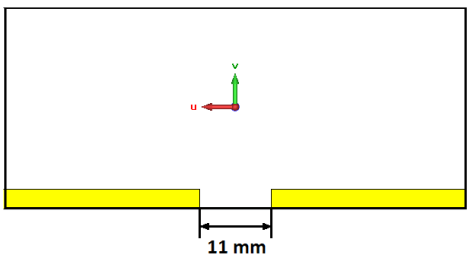

(b) Bottom view

FIGURE 10. The proposed MIMO antenna

B. SIMULATION RESULTS AND ANALYSIS

1) REFLECTION COEFFICIENT AND MUTUAL COUPLING

The simulated results of reflection coefficients of the MIMO antenna without adjacent arcs are shown in Figure 11. From this figure, it is observed that the S11 parameter seems unchanged compared with the single antenna. At most of the operating bands, the S21 values are over -20dB due to close distance. Thus, it cannot meet the isolation demand for a good MIMO antenna [15]. To decrease mutual coupling at all operating bands in both switching states, the structure of adjacent arcs on the surface plane is placed between two antenna elements as shown in the previous section. The S21 value of MIMO antenna with and without decoupling structure are compared and illustrated in Figure 12.

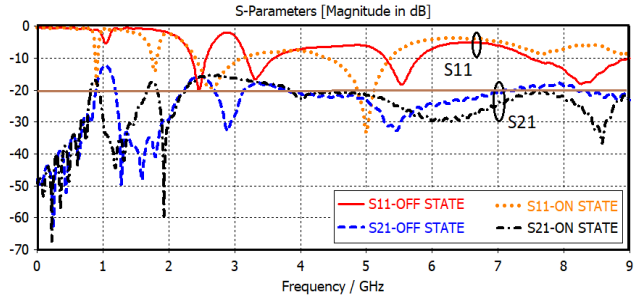

FIGURE 11. Simulated coefficient of the MIMO antenna without decoupling structure at different states

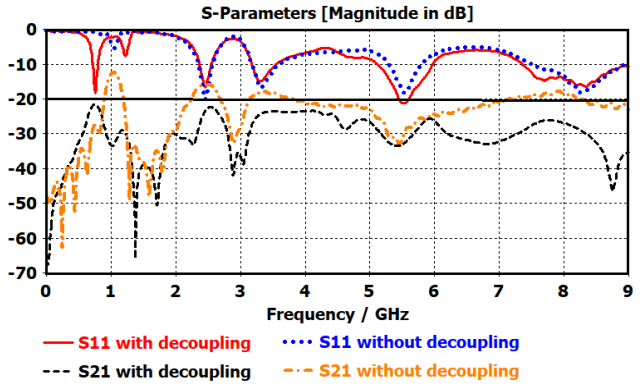

(a) OFF state

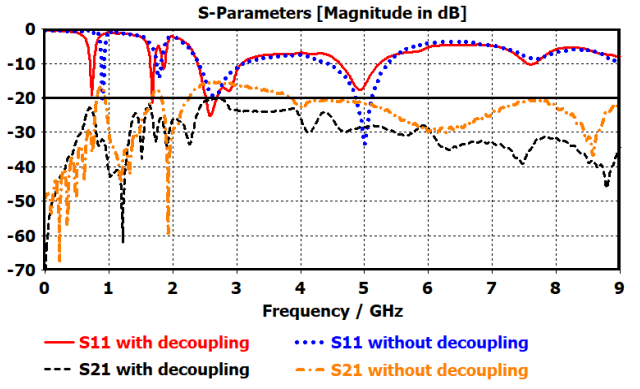

(b) ON state

FIGURE 12. Simulated coefficient of the MIMO antenna with/ without decoupling structure at different states

In OFF state, S21 decreases from -15dB down to -22dB at 2.4 band, from -17.5 down to -23.13dB at 3.3GHz band, and from -17.5dB down to -17dB at 7.8GHz resonant frequency. S21 gets a quite low value of -34.4dB at 5.5GHz band. We can see the same reduction of mutual coupling on the proposed MIMO antenna in the ON state. S21 reduces by just over 6dB and achieves the value of -22.5dB, -22dB, and -28dB at 900MHz, 1.8GHz, and 5GHz band, respectively. At 2.6GHz frequency, the value of S21 is just -20dB and gets a decrease of 5dB. Thus it can be seen that the gradient arc structure can reduce the mutual coupling between close elements in the MIMO antenna for wide bandwidth. The MIMO antenna with the proposed decoupling structure achieves the high isolation of over 20dB at all operating bands.

2) RADIATION PATTERN

Fig.13 shows the simulated radiation patterns of the proposed reconfigurable MIMO antenna at eight different resonant frequencies in two states. It is obvious that the same polarization is achieved in the MIMO antenna.

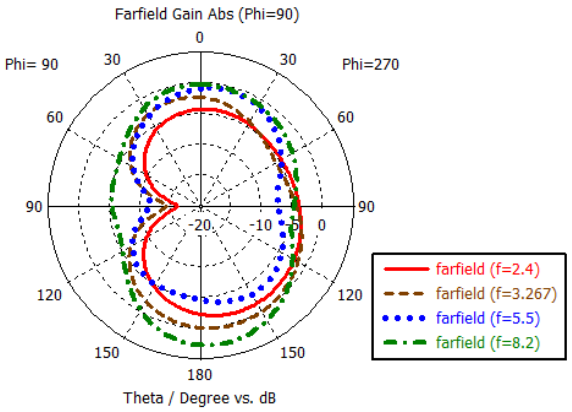

(a) OFF state

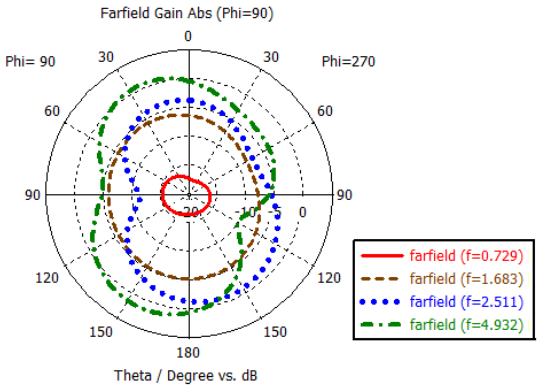

(b) ON state

FIGURE 13. Radiation pattern of the proposed MIMO antenna

3) ENVELOPE CORRELATION COEFFICIENT

In the MIMO antenna system, the correlation factor, which is called the envelope correlation coefficient (ECC), will be significantly degraded with higher coupling levels. This parameter can be calculated from radiation patterns or

scattering parameters. For a simple two-port network, assuming it is in a uniform multipath environment, the envelope correlation (ρ_e) can be calculated conveniently and quickly from S-parameters, as follows [16]:

$$\rho_e = \frac{|S_{11}^* S_{12} + S_{21}^* S_{22}|^2}{(1-|S_{11}|^2-|S_{21}|^2)(1-|S_{22}|^2-|S_{12}|^2)} \quad (11)$$

The correlation factor curve of the proposed MIMO antenna is shown in Figure 14. From this figure, the MIMO has simulated ECC lower than 0.005 for all operating bands. Therefore, it is quite suitable for wireless equipment with a value of $|\rho| \le 0.5$ for the bands of interest.

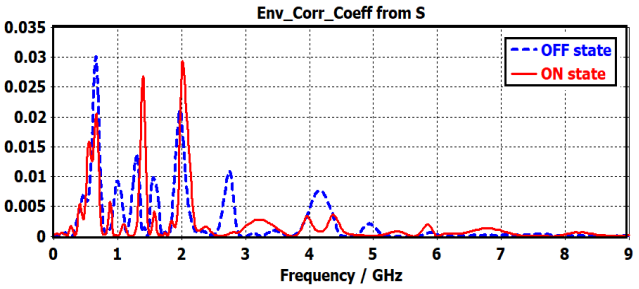

FIGURE 14. ECC curve of the proposed MIMO antenna

4) COMPARISON

TABLE V. Performance Comparison of the proposed MIMO antenna and recently published work

REF	Size (mm^3)	No of operating bands	Center Frequency (GHz)	Peak gain (dB)	Minimum isolation (dB)	Maximum ECC
[10]	32x98x1	6	0.6; 1.8; 2.4; 3.5; 4.2; 5.5	5.1	15	0.04
[11]	38x38x1.6	2	2.45; 5.4	2.8	15	0.2
[12]	100x50x1.5	6	1.48; 1.72; 1.9; 2.01; 2.14; 2.27	2.2	12	0.125
This work	30.78x71x1.6	8	0.73; 1.63; 2.45; 2.51; 3.31; 4.9; 5.5; 8.3	3.7	20	0.005

Table V provides a performance comparison of our design with previously reported frequency reconfigurable multi-band MIMO antennas in recent years. Their dimensions, operating bands, and peak gain as well as their corresponding minimum isolation and maximum ECC are compared. It can be observed that our design has a good trade-off between miniaturization rate and performance. Moreover, it achieves high isolation at all of eight operating bands so we can apply the proposed antenna design as well as the structure of the gradient arcs for applications in mobile equipment of modern communication systems in IoT era.

C. MEASUREMENT

Fabricated on the FR4 substrate, the measured results of the S parameter are compared with simulated ones as illustrated in Fig. 15.

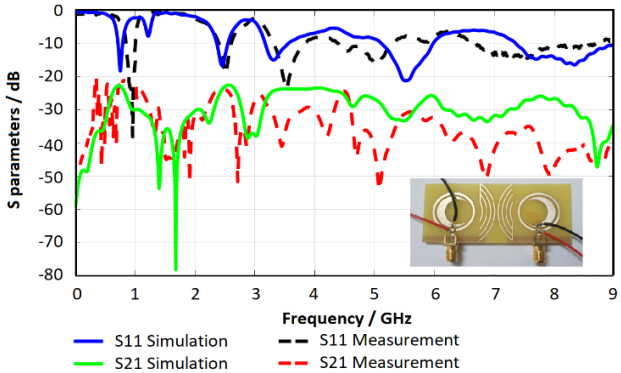

(a) OFF state

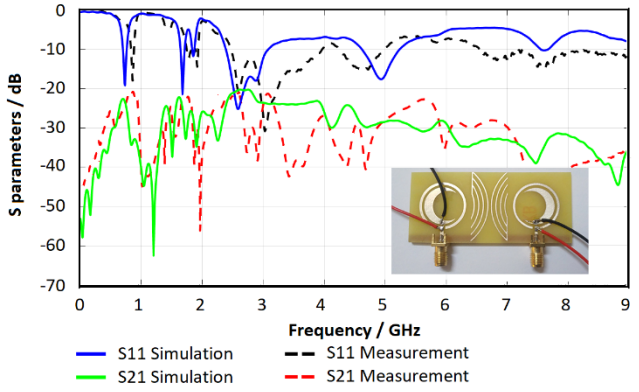

(b) ON state

FIGURE 15. Measured antenna with decoupling structure

From the plot, one can observe that the measured and simulated results display a fair agreement to validate the effect of the proposed structure

IV. CASE STUDY: USING THE PROPOSED ANTENNA FOR USB WIFI ADAPTER

A. TEST CONFIGURATION

To verify the performance of the proposed antenna in a realistic environment, the antenna is used with a USB Wi-Fi adapter to test the 2.4GHz band. This is one of the main frequencies in both IEEE 802.11 and IoT communication. Shown in Fig.16 is the test set up. It includes:

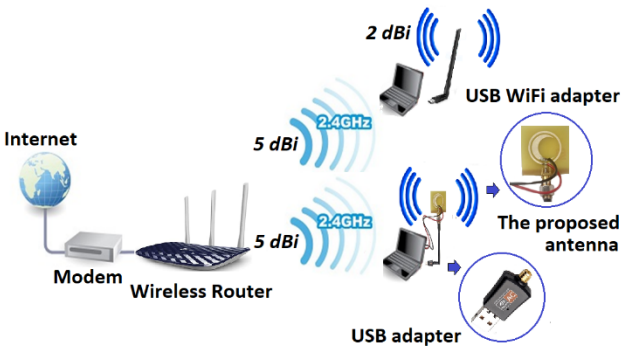

FIGURE 16. Test set up of the proposed antenna

- A wireless router that can establish a live connection to the PC/ laptop, is connected to an antenna on the USB Wi-Fi adapter. Here, we use a Wireless Router TP-Link Archer C20 whose transmit power is 19dBm, the transmitting gain is 5dBi.
- A USB Wi-Fi Adapter for PC/ Laptop that contains a USB adapter and a dipole antenna. The Adapter connects to PC/ Laptop via USB port and to Wireless router via antenna whose has a receiver sensitivity from -110dBm to -40dBm and 2dBi gain.
- The proposed antenna that connects to PC/ Laptop via USB Adapter AC600.
- A PC/ Laptop has installed Wi-Fi Analyzer Application.

B. EXPERIMENTAL RESULT

All test process is undertaken in an environment containing obstacles. The experimental result is achieved from Wi-Fi Analyzer software and shown in Fig. 17 and Fig.18.

(a) At a distance of 15m

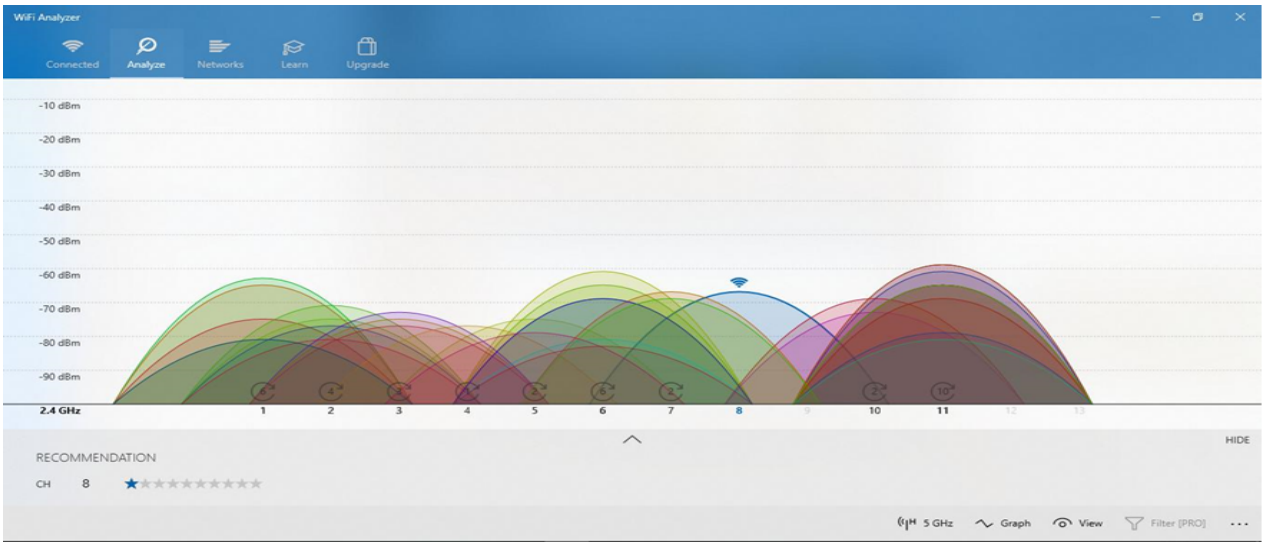

(b) At a distance of 55m

FIGURE 17. The receiver signal strength of the proposed antenna

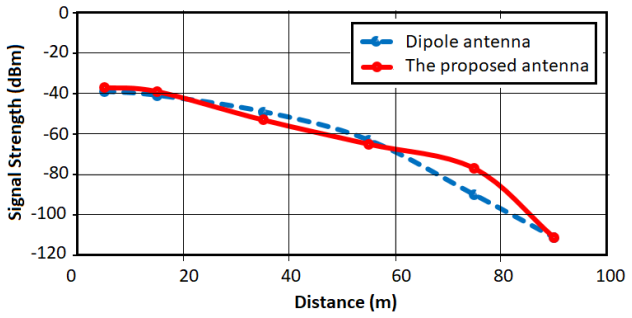

FIGURE 18. The signal strength comparison of the proposed antenna and the dipole antenna

One can observe that the USB adapter with the proposed antenna can receive signals quite well. Compared with the dipole antenna of Wi-Fi USB Adapter AC, the receive signal strength is the same. At a close distance of above 20m and long-distance of over 60m, the proposed antenna can get the Wi-Fi signal a bit better.

V. CONCLUSION

In this paper, a novel frequency reconfigurable quad-band antenna is proposed. Based on a complex structure of ring shape and new moon one, the antenna has a compact size of 30x30 mm^2 at a low frequency of 900MHz. Thanks to a novel structure of gradient arcs, the MIMO antenna achieves a low mutual coupling which is under -20dB for all eight operating bands from 750 MHz to 9GHz. Additionally, the proposed single antenna is tested with a Wi-Fi USB Adapter and achieves a good signal strength to validate the effect of the proposed structure in a live 802.11 system as well as IoT communication.

REFERENCES

[1] Saravana, M.J.S. Rangachar, "Polarization Reconfigurable Square Patch Antenna for Wireless Communications," *Advanced Electromagnetics*, vol. 7, no. 4, pp. 103-108, Sep. 2018.

[2] N. O. Parchin, H. J. Basherlou, Y. I.A Al-Yasir, R. A. Abd-Alhameed, A. M.Abdulkhaleq, and J. M.Noas, "Recent Developments of Reconfigurable Antennas for Current and Future Wireless Communication Systems," *Electronics*, vol.8, no.2, 128, 17 pages, Feb. 2019.

[3] Tayyaba Khan, MuhibUr Rahman, Adeel Akram, Yasar Amin and Hannu Tenhunen, "A Low-Cost CPW-Fed Multiband Frequency Reconfigurable Antenna for Wireless Applications," *Electronics*, vol.8, no.8, 900, 17 pages, Aug. 2019.

[4] Jayendra Kumar, Banani Basu, Fazal Ahmed Talukdar, Arnab Nandi, "Stable-multiband frequency reconfigurable antenna with improved radiation efficiency and increased number of multiband operations," *IET Microwave, Antennas & Propagation*, vol. 13, Iss.5, pp. 642-648, 28th February 2019.

[5] Hattan F. Abutarboush, and A. Shamim, "A Reconfigurable Inkjet Printed Antenna on Paper Substrate for Wireless Applications," *IEEE Antennas and Wireless Propagation Letters*, vol.17, issue.9, pp.1648-1651, September 2018.

[6] Saffrine Kingsly, Deepa Thangarasu, Malathi Kanagasabai, M.Gulam Nabi Alsath, T.Rama Rao, P. Sandeep Kumar, Yogeshwari Panner Selvam, Sangeetha Subbaraj, Padmathilagam Sambandam, "Multiband Reconfigurable Filtering Monopole Antenna for Cognitive Radio Applications," *IEEE Antennas and Wireless Propagation Letters*, vol.17, issue.8, pp.1416-1420, August 2018.

[7] A Vamseekrishna, B T P Madhav, T Anilkumar, L S S Reddy, "An IoT controlled octahedron frequency reconfigurable multiband antenna for microwave sensing applications," *IEEE Sensors Letters*, vol. 2(3), 2019.

[8] V. Arun and L.R. Karl Marx, "Internet of Things Controlled Reconfigurable Antenna for RF Harvesting,", *Defense Science Journal*, vol. 68, pp. 566-571, No. 6, November 2018.

[9] G. Irene and A. Rajesh, "Review on the Design of the Isolation Techniques for UWB MIMO Antennas," *Advanced Electromagnetics*, vol.7, no.4, pp.46-70, Aug. 2018.

[10] M. M. Hassan, Z. Zahid, A. A. Khan, I. Rashid, A. Rauf, M. Maqsood, and F. A. Bhatti, "Two elements MIMO antenna with frequency reconfigurable characteristics utilizing RF MEMS for 5G applications," *Journal of Electromagnetic Waves and Applications*, vol.34, issue.9, pp.1210-1224, May 2020.

[11] S. R. Thummaluru, R. Kumar, R. K. Chaudhary, "Isolation and frequency reconfigurable compact MIMO antenna for wireless local area network applications," *IET Microwaves, Antennas and Propagation*, vol.13, issue.4, pp.519-525, 2019.

[12] S. Riaz, X. Zhao, S. Geng, "A frequency reconfigurable MIMO antenna with agile feed line for cognitive radio application," *International Journal of RF and Microwave Computer-Aided Engineering*, 9 pages, Dec. 2019.

[13] M.S.Shakhirul, M.Jusoh, Y.S.Lee and C.R.Nurol Husna, "A Review of Reconfigurable Frequency Switching Technique on Microstrip Antenna," 1st International Conference on Green and Sustainable Computing, *Journal of Physics*: Conf. Series 1019, 2018.

[14] Ramesh Grag, Prakash Bhartia, Inder Bahl, Apisak Ittipiboon, "Microstrip Antenna Design Handbook," Artech House, *Antennas and Propagation Library*, 2001.

[15] Istvan Szini, Alexandru Tatomirescu, and Gert Frølund Pedersen, "On Small Terminal MIMO Antennas, Harmonizing Characteristic Modes with Ground Plane Geometry," *IEEE Antenna Propag. Trans. On*, vol. 63, no. 4, pp.1487 - 1497, 2015.

[16] A. Lai, K.M.K.H. Leong, and T.Itoh, "Infinite Wavelength Resonant Antennas with Monopole Radiation Pattern Based on Periodic Structures," *IEEE Trans. Antennas Propag.*, vol.55, no.3, pp.868-876, Mar 2007.